

Original Article

# Design and Study of Voltage-Dependent Capacitor Using BJT and Its Application as A Reactance Modulator

Binoy Das<sup>1</sup>, Moumita Patra<sup>1</sup>, Julekha Khatun<sup>2</sup>, Atindra Nath Pal<sup>3</sup>, Bipan Tudu<sup>4</sup>, Nityananda Das<sup>1\*</sup>

<sup>1</sup>Department of Physics, JK College, Purulia, India.

<sup>2</sup>Nanomaterials Research Lab, Department of Chemistry, Sidho-Kanho-Birsha University, Purulia, India.

<sup>3</sup>Satyendra nath bose national centre for basic sciences, Salt Lake, Kolkata, India.

<sup>4</sup>Department of Instrumentation and Electronics Engineering, Jadavpur University, Salt Lake City, Kolkata, India.

\*Corresponding Author : [ndas228@yahoo.com](mailto:ndas228@yahoo.com)

Received: 10 March 2025

Revised: 15 April 2025

Accepted: 28 April 2025

Published: 31 May 2025

**Abstract** - Amplitude and frequency modulation, along with the design of oscillators, and tank circuits, are fundamental components of communication systems. A critical aspect of frequency modulation is a comprehensive understanding of reactance modulators and their operational limitations. In this study, we experimentally investigated the performance of a reactance modulator using a Bipolar Junction Transistor (BJT, 2N3904). We analyse the variation of transconductance as a function of the base-emitter voltage and demonstrate the linearity of the equivalent capacitance across different input base-emitter voltages. Base-emitter voltages varied from 0.5 volts to 0.75 volts, and the corresponding equivalent capacitance of the reactance modulator was observed to be 0.35 pF to 4273.34 pF, respectively. Frequency modulation with a 220 kHz carrier signal was studied using a Hartley oscillator. The experimental results showcase the effectiveness of employing a BJT as a reactance modulator for achieving frequency modulation, highlighting its potential applications in communication systems.

**Keywords** - BJT, Equivalent capacitance, Frequency Modulation, Reactance modulator, Transconductance.

## 1. Introduction

In the past few decades, the advancement of analog and digital communication systems through worldwide has continually emphasised the importance of effective modulation techniques, which are essential for transmitting information efficiently across various media [1-3]. Among the different modulation techniques, the basic methods are amplitude, frequency, and phase modulations to realise data transmission in communication systems, and particularly Frequency Modulation (FM) is valued for its resilience to noise and its extensive applications in broadcasting, signal processing, and telecommunications [4-7]. Edwin Howard Armstrong was the pioneer who, in 1933, successfully demonstrated FM transmission [8].

Precise and efficient frequency variation is the key factor in the generation of FM signals. The basic idea of frequency modulation is the change of the resonance frequency of a tank circuit composed of a capacitor and an inductor, with the variation of the amplitude of the message signal. This requires a capacitance that varies linearly with the amplitude of the message signal. L. J. Giacoletto, in his work [9], had shown the variation of capacitance of a junction semiconductor with bias voltage. M.H. Norwood et al. and H. Funato et al. discussed the voltage variable capacitor [10, 11]. Varactor

diode with its properties can be utilized to change the capacitance with input bias voltage [12-15]. However there are limitations on the use of a varactor diode. This can be overcome by using a reactance modulator with its special circuitry [16].

A reactance modulator operates by varying the reactance of a circuit to change the frequency of the carrier signal and, hence, is particularly effective in generating FM signals [17]. Among the various implementations of reactance modulators, those utilizing Bipolar Junction Transistors (BJTs) are prominent due to the favourable electrical characteristics of BJTs, such as high gain, stability, and ease of integration into existing circuit designs [18-19].

The utilization of BJTs in reactance modulators takes advantage of the transistor's ability to vary its reactance in response to changes in the base-emitter voltage, which in turn modulates the frequency of the output signal based on the input modulating signal. This modulation mechanism is fundamental to generating FM signals with high fidelity and precision. In M B Chowdary et al. [20], frequency modulation was realized using BJT. However, the variation of equivalent capacitance with input voltages, the operating zone of the BJT, is essential in the application of the BJT as a reactance



modulator in an FM circuit. Colpitts [21] or Hartley oscillators [22-23] are commonly used to generate carrier frequencies. The basic requirements for their operation include the oscillation startup criterion and a stable frequency condition to ensure smooth performance [24-26]. In classroom teaching, these theories are usually taught in lecture mode, and in practical classes, an experimental kit is used to demonstrate these fundamental concepts.

In experimental kits, all the components are predefined, which leaves very little opportunity to vary the modulating or carrier signals. Consequently, users may not observe differences, leading to a lack of learning. The analysis provided in this study offers valuable insights into the design and optimization of reactance modulators and the design of the Hartley oscillator, contributing to a deeper understanding of FM technology and its ongoing significance in modern communication systems.

In this paper, we have experimentally demonstrated the FM generation employing a BJT-based reactance modulator. Precise and efficient FM was achieved using the Hartley Oscillator as a carrier signal generator. We have analytically explained the use of BJT as a square-law device.

The linear variation of equivalent capacitance with the Base-Emitter voltage has been theoretically and experimentally studied. The range of capacitance for different feedback capacitors is reported. The variation of transconductance in different regions of the transfer characteristics of a BJT is experimentally demonstrated.

## 2. Theoretical Analysis

Any sinusoidal signal can be expressed as,

$$v = A \cos(\omega t)$$

Where  $A$  is the amplitude of the signal and  $\omega$  is the angular frequency. In different modulation methods, such as amplitude modulation, the amplitude of the carrier signal varies according to the modulating signal where, whereas in frequency modulation angular frequency varies with the modulating signal. In amplitude modulation, the amplitude is transformed as

$$A = V_c + V_m \cos \omega_m t = V_c \left( 1 + \frac{V_m}{V_c} \cos \omega_m t \right)$$

Where,  $v_m = V_m \cos \omega_m t$  is the modulating signal, and  $V_c$  is the amplitude of the carrier signal. In Frequency modulation, the angular velocity ( $\omega$ ) of the carrier signal varies according to the amplitude of the modulating signal

$$\omega = \omega_c + k_f V_m \cos \omega_m t$$

Where,  $k_f V_m$  is the degree of frequency variation proportional to the modulating amplitude. Thus, the modulated signal will be

$$v = V_c \cos \left( \omega_c t + \frac{k_f V_m}{\omega_m} \sin \omega_m t \right) = V_c \cos \left( \omega_c t + m_f \sin \omega_m t \right), \quad m_f = \frac{k_f V_m / 2\pi}{f_{m\max}} = \frac{\Delta f_{\max}}{f_{m\max}}$$

The frequency deviates from the centre frequency in proportion to the amplitude of the modulating signal. Using mathematical analysis, the modulated signal can be represented as

$$v = V_c \{ J_0(m_f) \cos \omega_0 t - J_1(m_f) [\cos(\omega_0 - \omega_m)t - \cos(\omega_0 + \omega_m)t] + J_2(m_f) [\cos(\omega_0 - 2\omega_m)t + \cos(\omega_0 + 2\omega_m)t] \dots \} \quad [5]$$

Where  $J_n$ , coefficients of Bessel functions of the first kind and order  $n$ .

Thus, a frequency-modulated wave has a centre frequency  $f_0 = \omega_0 / 2\pi$  and an infinite set of side frequencies, each pair spaced by an amount equal to the modulating frequency and its integral multiples.

### 2.1. Block Diagram of FM

An FM signal can be realised by varying the capacitance of a tuned oscillator. The variation of the capacitance must be according to the modulating signal, i.e. vary linearly with the control voltage. The schematic diagram of a frequency-modulated signal is shown in Figure 1.

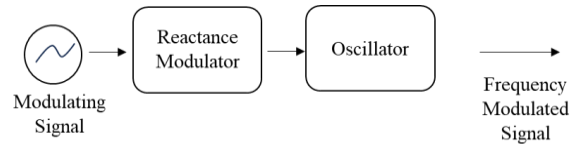


Fig. 1 Block diagram of frequency modulation

The modulating signal is fed into the reactance modulator, and the equivalent capacitance of the reactance modulator changes according to the modulating signal. The output of the reactance modulator is connected to the oscillator. The transistor-based or FET-based voltage-biased reactance circuits are often used in frequency modulation as an effective method for varying frequency in accordance with the message signal.

### 2.2. Transistor-Based Reactance Modulator

In this study, the variation of the capacitance of a reactance modulator is studied so that this reactance modulator can be used as a voltage-dependent capacitor for frequency modulation and demodulation.

This includes a proper understanding of impedance, the range of capacitance variation, and the range of voltage variation to be applied. The schematic diagram of the reactance modulator based on the BJT transistor (2N3904) is shown in Figure 2.

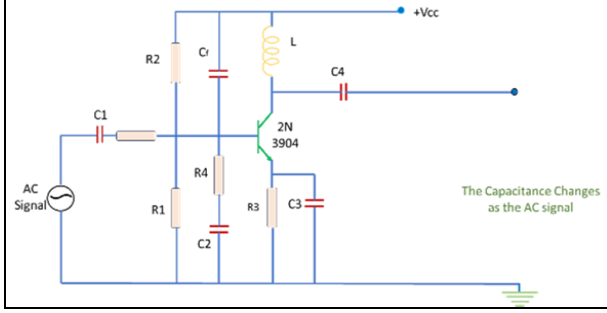


Fig. 2 Schematic diagram of reactance modulator using BJT transistor

In this scheme, the reactance modulator is in common-emitter mode. Two resistors, one in base to emitter (R1) and the other in collector to base (R2), provide the required biasing for the transistor. Condition for reactance modulator is fulfilled by employing a capacitor in between collector and base of the transistor known as feedback capacitor ( $C_f$ ) and a resistor in between base to emitter resistor ( $R_4$ ) known as emitter feedback resistance. Two capacitors,  $C_1$  and  $C_4$ , are used as coupling capacitors, and  $C_3$   $R_3$  are bypass capacitors and emitter feedback resistors, respectively.

In a transistor, the relation between collector current ( $I_C$ ) and base-emitter ( $V_{BE}$ ) voltage is

$$I_C = I_S(e^{V_{BE}/V_T} - 1) \quad (1)$$

Where  $I_S$ , Saturation current, and  $V_T$  is the Thermal voltage. Equation 1 shows that the collector current varies exponentially with the base-emitter voltage ( $V_{BE}$ ), and its experimental verification is shown for 2N3904 BJT in Figure 3 with exponential fitting (red line).

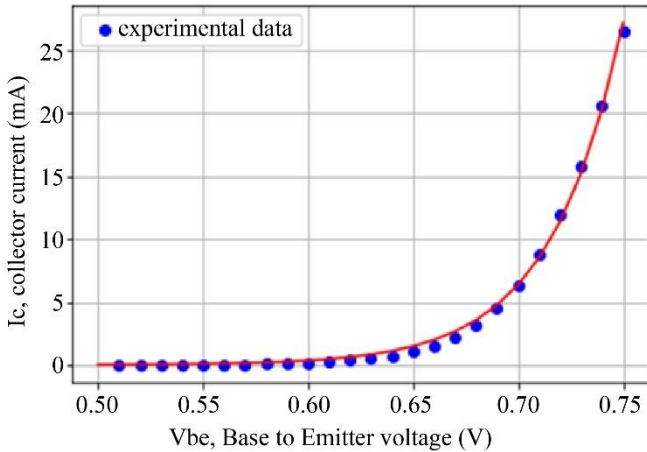


Fig. 3 Transfer characteristics of the transistor ( $I_C$  vs  $V_{BE}$ ).

Introduction of the AC signal voltage to the input of the transistor, the expression for collector current, Equation 1, becomes

$$I_C = I_S(e^{(V_{BE}+V_a)/V_T} - 1) \quad (2)$$

where  $V_a$  is the effective change in base-emitter voltage due application of the input AC signal.

From elementary algebra,

$$\exp(x_0 + x) = 1 + (x_0 + x) + \dots$$

Thus, after the expansion of equation 2, it becomes

$$I_C = I_S \left( 1 + \frac{V_{BE} + V_a}{V_T} + \left( \frac{V_{BE} + V_a}{V_T} \right)^2 \frac{1}{2!} + \frac{1}{3!} \left( \frac{V_{BE} + V_a}{V_T} \right)^3 \dots - 1 \right)$$

After rearranging, the expression becomes

$$I_C = I_S \left( 1 + \frac{V_{BE} + V_a}{V_T} + \left( \frac{V_{BE}^2 + 2V_{BE}V_a + V_a^2}{V_T^2} \right) \frac{1}{2!} + \left( \frac{V_{BE}^3 + 3V_{BE}^2V_a + 3V_{BE}V_a^2 + V_a^3}{V_T^3} \right) \frac{1}{3!} \dots - 1 \right)$$

or

$$I_C = I_S \left( V_a \left( \frac{1}{V_T} + \frac{2V_{BE}}{V_T^2} \frac{1}{2!} + \frac{3V_{BE}^2}{V_T^3} \frac{1}{3!} + \dots \right) + V_a^2 \left( \frac{1}{V_T^2 2!} + \frac{3V_{BE}}{V_T^3} \frac{1}{3!} + \dots \right) + \dots + \left( \frac{V_{BE}}{V_T} + \frac{V_{BE}^2}{V_T^2 2!} + \dots \right) \right)$$

or

$$I_C = I_S(V_a A + V_a^2 B + \dots + K) \quad (3)$$

Where,  $A = \left( \frac{1}{V_T} + \frac{2V_{BE}}{V_T^2} \frac{1}{2!} + \frac{3V_{BE}^2}{V_T^3} \frac{1}{3!} + \dots \right)$   $B = \left( \frac{1}{V_T^2 2!} + \frac{3V_{BE}}{V_T^3} \frac{1}{3!} + \dots \right)$  and  $K = \left( \frac{V_{BE}}{V_T} + \frac{V_{BE}^2}{V_T^2 2!} + \dots \right)$

$V_{BE}$  is constant for a particular biasing arrangement of the BJT, and  $V_T$  also remains constant in thermal equilibrium. Hence, A, B, and K are constants. Equation 3 expresses the variation of collector current with base-emitter voltage. By judicious choice of  $V_{BE}$ , the collector current ( $I_C$ ) can be a second-order polynomial of  $V_a$  and can be utilized as a square law device. Differentiating equation 3 with respect to  $V_a$

$$g_m = \frac{\partial I_C}{\partial V_a} = I_S(A + 2V_a B + \dots) \quad (4)$$

where  $g_m$  is the transconductance of the BJT. Thus, the transfer characteristic follows an exponential variation with the base-emitter voltage. If the base-emitter junction is biased in such a way that the collector current, which is a function of base-emitter voltage, obeys equation 3, then in this particular operating region, the transfer characteristic follows a square law and the transconductance,  $g_m$ , of the transistor, varies linearly with the applied base voltage as expressed by equation 4 and shown in Figure 4.

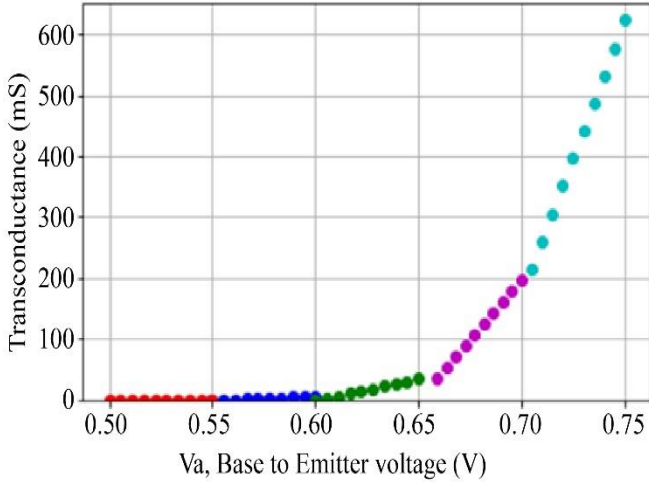


Fig. 4 The graph of transconductance vs base-emitter voltage ( $V_a$ ) for different regions.

Thus, the reactance modulator exploits the piecewise square law behaviour of a transistor transimpedance. As a whole, the transfer characteristic of a BJT follows an exponential rise, but this can be treated as a piecewise square law behaviour. For a particular region, the I-V characteristic is approximated as a square law behaviour to a sufficient accuracy. The square law behaviour of I-V leads to the linear behaviour of transimpedance.

The nature of the graph, Figure 4, reveals that the graph is piece-wise linear, and the value of the transconductance depends on the region of choice of the base-emitter voltage. The equation of the graph for any such region can be expressed as

$$g_m = mV_a + c \quad (5)$$

where ‘m’ is the slope of the line at the corresponding region and ‘c’ is the intercept point. If the DC biasing of the transistor provides DC base-emitter voltage  $V_{BE}$  and an ac input signal,  $V_0 \sin(\omega t)$ , is applied as shown in Figure 2, then the total base-emitter voltage becomes

$$V_a = V_{BE} + kV_0 \sin(\omega t).$$

Where ‘k’ is the fraction of the voltage that is fed into the base point. Thus, the expression of the transconductance, equation 5, becomes

$$g_m = m (V_{BE} + kV_0 \sin(\omega t)) + c.$$

and the equivalent capacitance of the device becomes

$$C_{eq} = g_m C_f R_4 \quad (6) [4]$$

Where  $C_f$  and  $R_4$  are feedback capacitance and emitter feedback resistance, respectively, thus, from the above analysis, it is found that depending on the region of operation, i.e.,  $V_{BE}$  and the input signal, the value of  $g_m$  and hence the

equivalent capacitance varies linearly with the input signal. Figure 5 shows the variation of capacitance with DC-bias voltage for three different feedback capacitors.

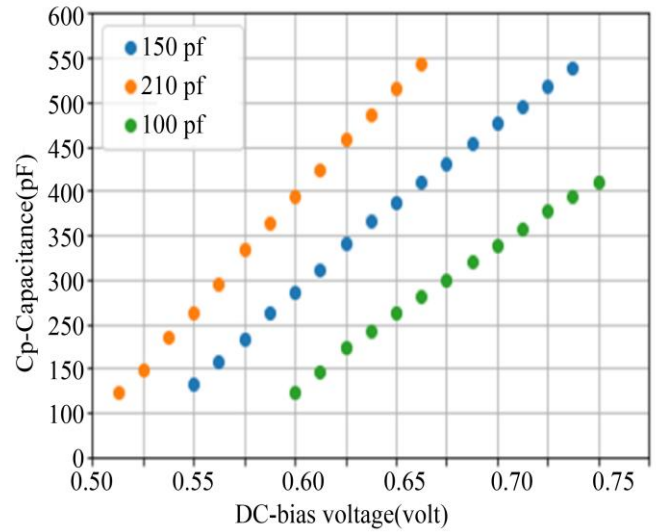


Fig. 5 Equivalent Capacitance of BJT vs applied DC-bias voltage for feedback capacitors 100 pF, 150 pF, and 210 pF.

In the case of the varactor diode (NTE 618), the variation of capacitance with DC bias is shown in Figure 6. The capacitance variation of the varactor diode with DC bias voltage is nonlinear, while the transconductance, hence the equivalent capacitance of the BJT, is also not linear over the whole region.

In the range of 1 volt to 5 volts,  $C_{max}$  is 512 pF, and  $C_{min}$  is 93 pF; hence, the capacitance ratio is (Capacitance ratio =  $C_{max} / C_{min}$ ) is 5.5, while in the case of BJT, the capacitance ratio for different regions of base-emitter voltage is different, as shown in Table 1. The value of  $C_{max}$  and  $C_{min}$  of the BJT-based reactance modulator can be varied by changing the feedback capacitor.

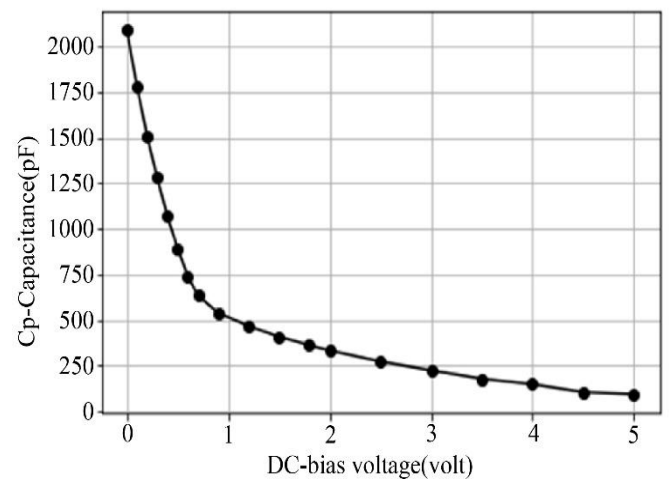


Fig. 6 Equivalent Capacitance of Varactor Diode vs applied DC-bias voltage

2.3. Transfer characteristics for FET(BS170)

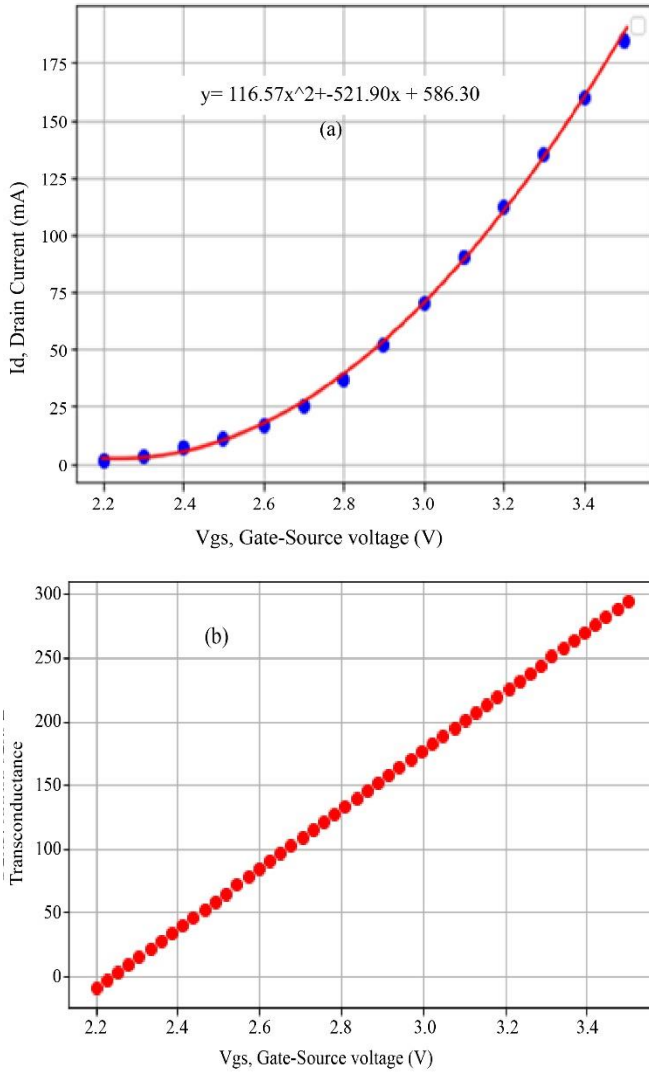


Fig. 7 (a) Change in drain current with Gate-Source voltage of FET(BS170), (b) Variation of transconductance with Gate-Source voltage of FET(BS170)

Figures 7(a) and 7(b) represent the drain current vs Gate-Source voltage and transconductance vs Gate-Source voltage, respectively, for BS170 MOSFET. In Figure 7(a), the nature of the graph shows that up to the drain current 175 mA, the device remains as a square-law device, and hence, the transconductance varies linearly with the Gate-Source voltage as shown in Figure 7(b). Therefore, using FET in a reactance modulator, the equivalent capacitance of the device will be linear to the input voltage.

Hence, the key point of capacitance variation with respect to the applied voltage to the base is the nonlinearity of the transfer characteristic of a BJT or FET. Figures 8(a) and 8(b) show variations of system capacitance with DC-bias voltage for FET and BJT, respectively. The standard deviation of  $C_p$

of FET is 301.209, and of BJT is 76.256; thus, BJT is more linear with input voltage than FET.

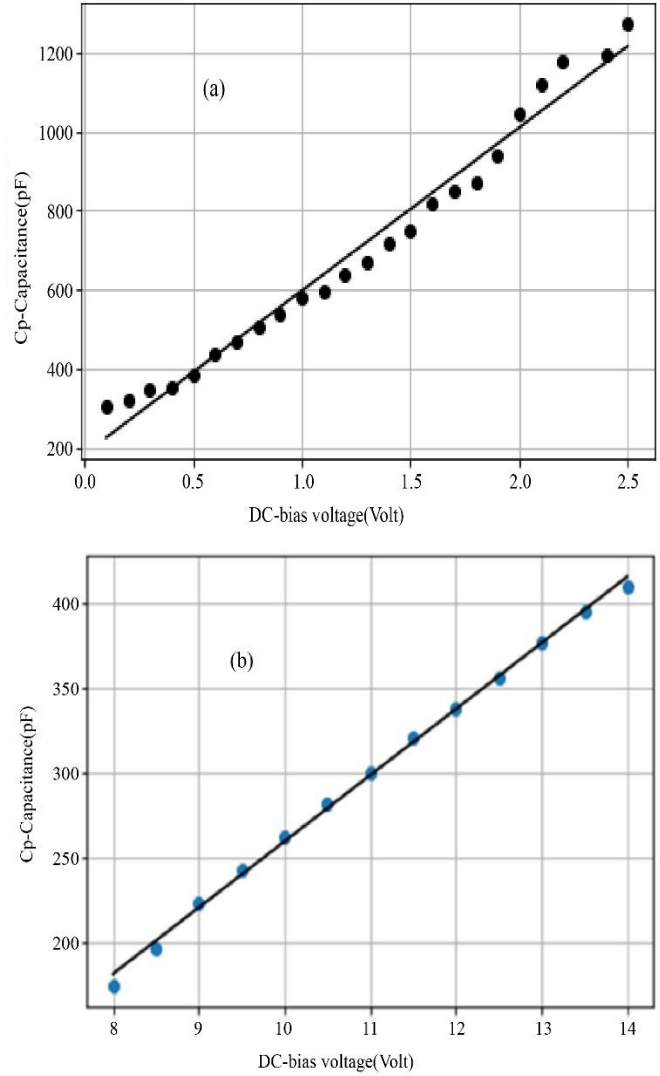


Fig. 8 Variation of equivalent capacitance with DC-bias voltage for (a)FET, (b) BJT

3. Results

3.1. The Linear Variation of Equivalent Capacitance with the Base-Emitter Voltage

The equivalent capacitance of the reactance modulator, Figure 9, was measured using a precision LCR meter (Tonghui make model TH2829A). The input AC signal was 100 milli Hz and  $V_{pp}$  2V.

The frequency of the LCR meter for this measurement was kept at 300 kHz. The feedback capacitance and emitter feedback resistance were 104.5 pF and 112.7Ω, respectively. The variation of equivalent capacitance is shown in Figure 9 for  $V_{BE}$  0.69 V. It was found that the equivalent capacitance was nicely sinusoidal according to the input sinusoidal signal. Thus, the linearity between input and output was observed.

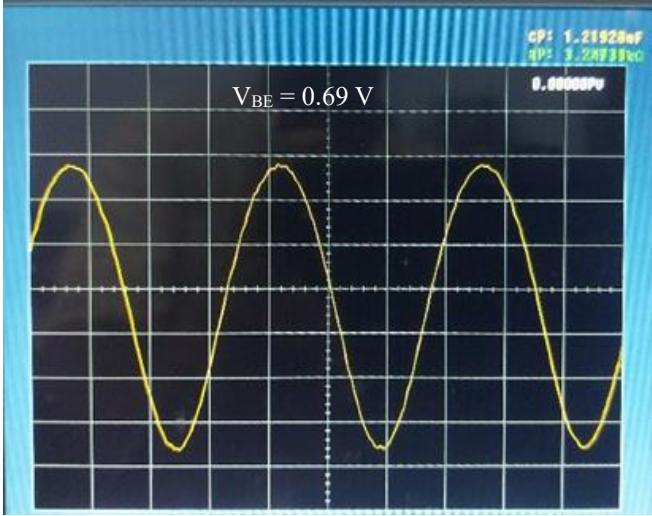


Fig. 9 Output of the LCR meter, equivalent capacitance for base-emitter voltage 0.69 V

### 3.2. Analytical Verification of Linearity between Input and Output and Equivalent Capacitance Calculation

Figure 10(a) shows the output of the function/arbitrary waveform generator (Siglent make, model SDG 810), which is the input signal to the reactance modulator. The peak-to-peak voltage of the signal was 2 V. The corresponding variation of equivalent capacitance from the machine data of the LCR meter is shown in Figure 10(b).

In this case,  $V_{BE}$  was 0.65 V. Figure 10(c) shows the point-to-point variation of equivalent capacitance with the given input voltage. The straight-line graph confirms the linearity between the input voltage and the corresponding equivalent capacitance.

From Figure 10(c), at the '0' input voltage, the equivalent capacitance is approximately 430 pF. The base-emitter voltage of this experiment was 0.65 volts, and the corresponding transconductance from Figure 4 is approximately 34.5 mS.

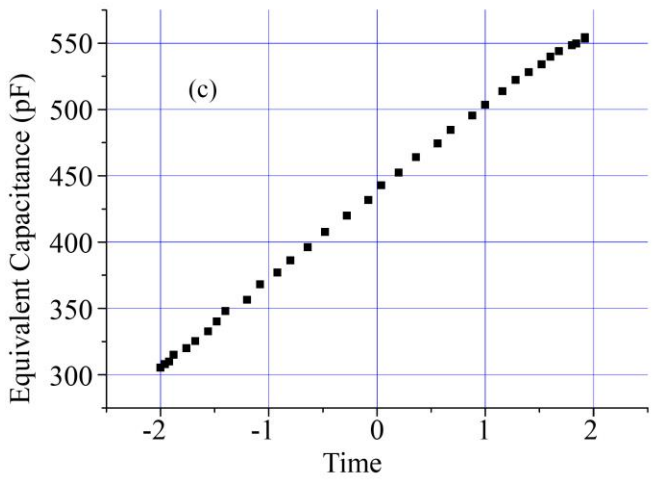
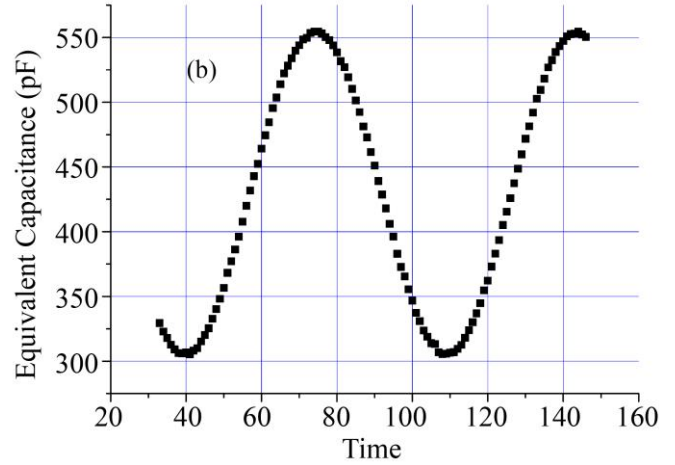
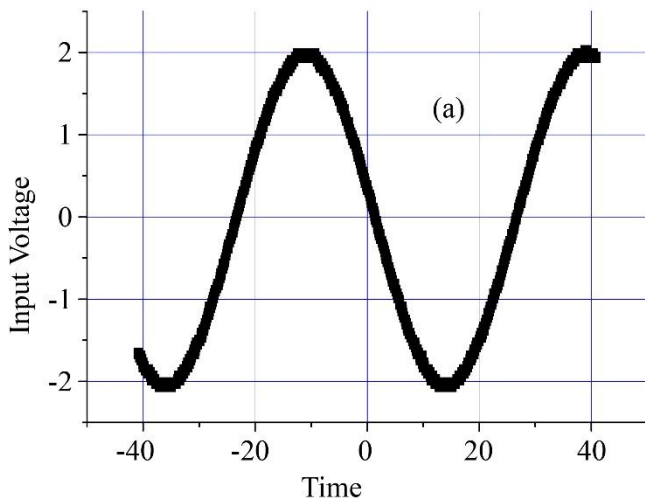


Fig. 10 (a) Variation of input voltage with time, (b) Variation of equivalent capacitance with time, (c) Graph for the variation of Equivalent capacitance with input voltage.

So, the calculated equivalent capacitance according to equation 5 is,

$$C_{eq} = 34.5 \times 10^{-3} \times 104.5 \times 10^{-12} \times 112.7 = 406.31 \text{ pF}$$

This is an excellent confirmation, considering the instrumental error.

The variation of equivalent capacitance for different regions in the transfer characteristics of the BJT for the feedback capacitance, 104.5 pF, and emitter feedback resistance, 112.7Ω, is depicted in Table 1.

### 3.3. Variation of Equivalent Capacitance with Different Input Voltages

The variation of equivalent capacitance for a 500 mV to 3 V (peak to peak) input signal is shown in Figure 11. For the base-emitter ( $V_{BE}$ ) voltage 0.70 V, it was found that the variation of equivalent capacitance was the exact replica of the input voltages, i.e., varying linearly with the input AC signal.

**Table 1. Variation of capacitance with Base-Emitter Voltage**

Base-Emitter Voltage (Va in Volt)	Capacitance (pF) Min	Capacitance (pF) Max	Difference (Max-Min)	Capacitance Ratio (C <sub>max</sub> /C <sub>min</sub> )
0.5 to 0.55	0.35	9.18	8.83	26.2
0.56 to 0.60	9.30	64.77	55.47	6.96
0.61 to 0.65	7.49	406.31	398.82	54.83
0.66 to 0.70	472.75	2330.11	1857.36	4.92
0.71 to 0.75	3062.88	7336.22	4273.34	2.39

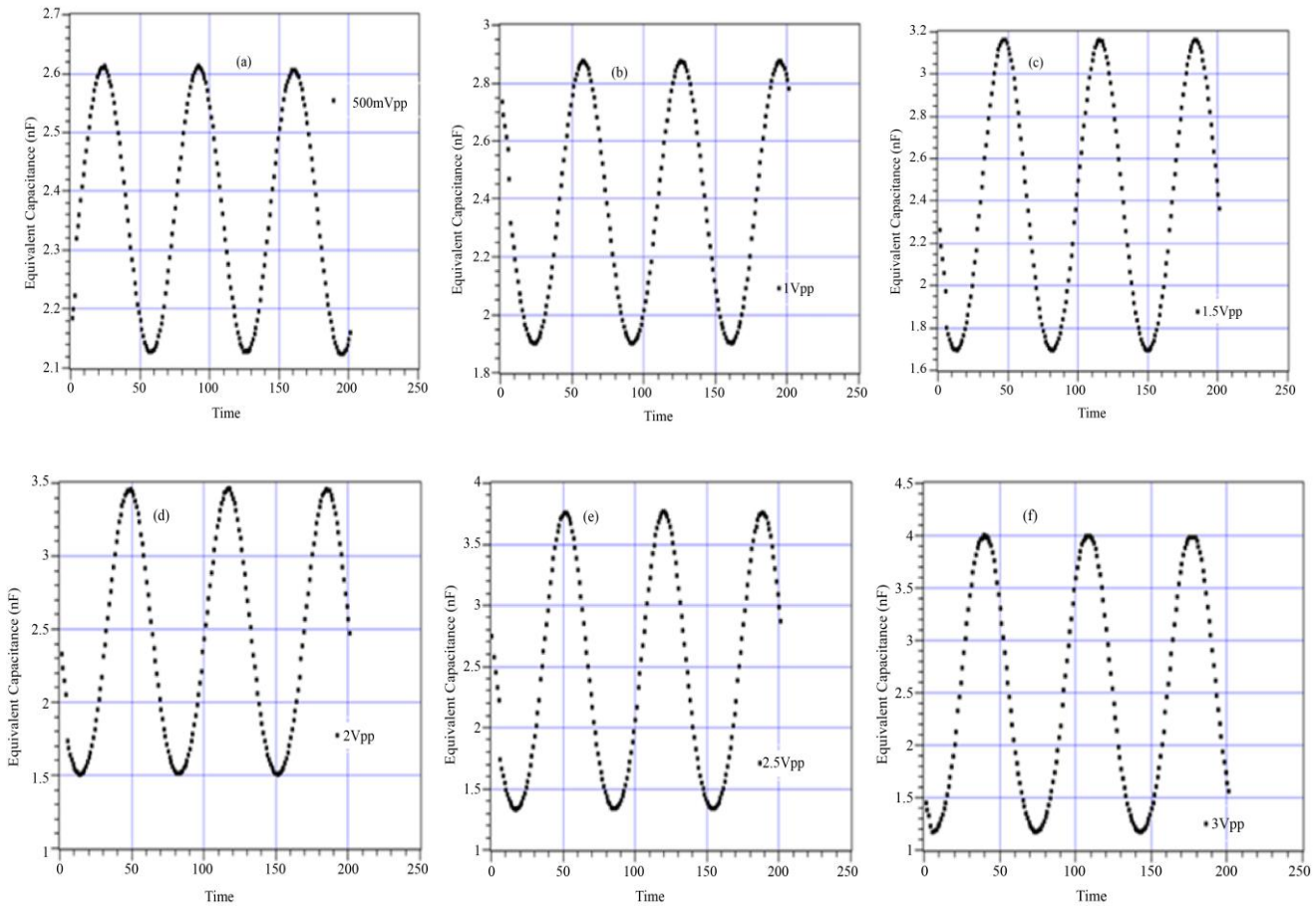


**Fig. 11** Equivalent capacitance for input voltages(peak-peak) (a)0.5 v (b)1 v (c) 1.5 v (d) 2 v (e) 2.5 v (f) 3 v.

**Table 2. Variation of equivalent capacitance with input voltages**

	1 V <sub>pp</sub>	2 V <sub>pp</sub>	3 V <sub>pp</sub>	4 V <sub>pp</sub>	5 V <sub>pp</sub>	6 V <sub>pp</sub>	7 V <sub>pp</sub>	8 V <sub>pp</sub>	9 V <sub>pp</sub>	10 V <sub>pp</sub>	11 V <sub>pp</sub>	12 V <sub>pp</sub>
Cp(pF) (mini)	494	482	472	447	426	414	395	382	370	361	346	332
Cp(pF) (max)	787	810	825	857	831	840	856	873	897	905	925	938

Table 2 shows the change in equivalent capacitance with input voltages for feedback capacitance 100.2 pF and emitter feedback resistance 96Ω. Figure 12 depicts the capacitance

ratio with input voltage, with a standard deviation of 0.3975, which conforms to its linearity. The maximum and minimum values of the capacitance can be altered by varying feedback capacitance and emitter feedback resistance.

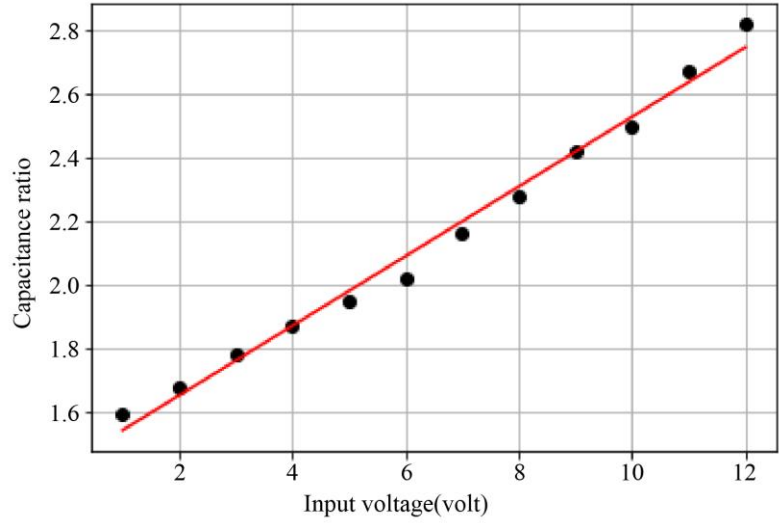


Fig. 12 Capacitance ratio for different Input Voltages

### 3.4. Experimental Arrangement for Harley Oscillator

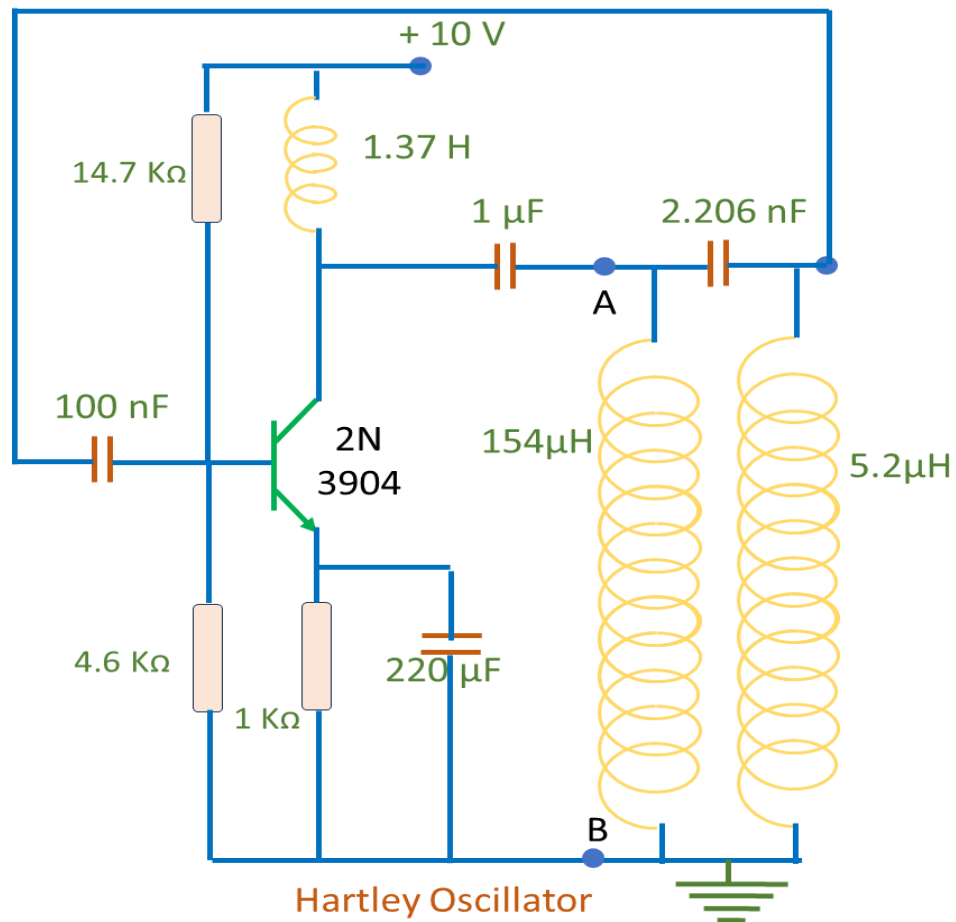


Fig. 13 Experimental diagram of the Hartley Oscillator.

The experimental arrangement of the Hartley Oscillator is shown in Figure 13. The tuned circuit consists of a capacitor of capacitance 2.206 nF and two inductors with inductance of

154 μH and 5.2 μH, as shown in the figure. The output of the oscillator is shown in Figure 14.

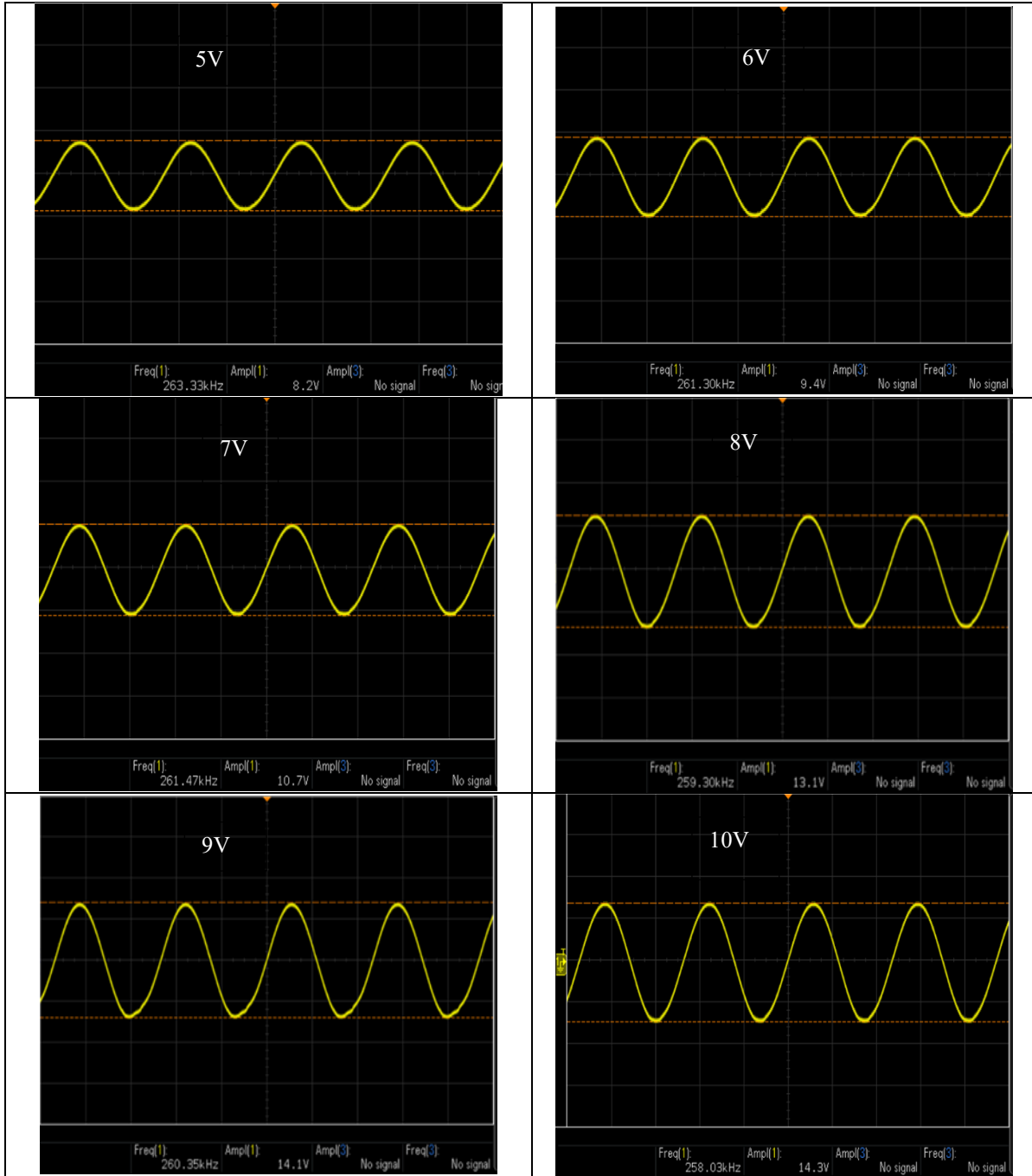


Fig. 14 Output of the Hartley Oscillator

It is observed that the frequency is approximately 260 kHz for different DC bias voltages, which confirms the frequency stability of the oscillator. The amplitude of the signal at DC bias volt 5V, 6V, 7V, 8V, 9V, 10V are 8.2V, 9.4V, 10.7V, 13.1V, 14.1V and 14.3V respectively.

**3.5. Experimental Arrangement for Frequency Modulation**

Figure 15 shows the circuit diagram for frequency modulation. The equivalent capacitance of the reactance

modulator using 2N3904 BJT changes linearly according to the input AC signal. This varying capacitor was fed into the tuned oscillator at points A and B (Figure 15), and frequency modulated output was observed.

The Hartley oscillator was used for the carrier signal. In this experiment, the tuned circuit of the Hartley oscillator was composed of a capacitor with a capacitance of 2.25 nF and two inductors with inductance  $L_1 = 240 \mu\text{H}$  and  $L_2 = 4.1 \mu\text{H}$ .

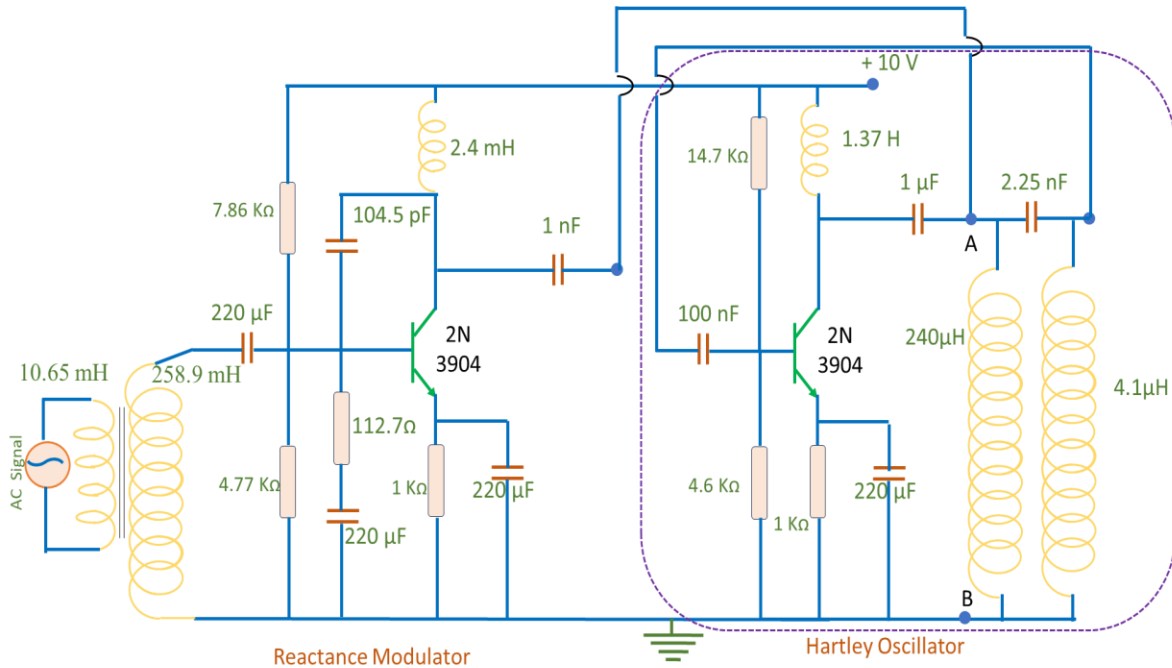


Fig. 15 Experimental arrangement of frequency modulation.

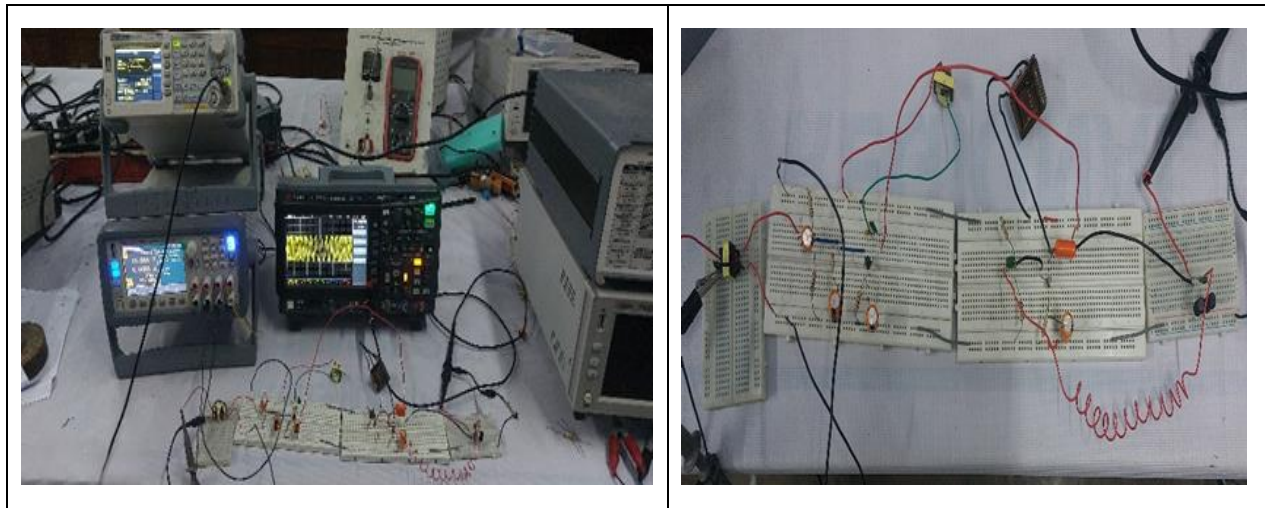


Fig. 16 Experimental setup of frequency modulation

The oscillation frequency of the tuned circuit of the Hartley Oscillator was

$$\frac{1}{2\pi\sqrt{LC}} \approx 220 \text{ kHz}$$

Where  $L = L_1 + L_2$  and  $C$  is the capacitance of the tuned circuit of the Hartley Oscillator. Thus, the Hartley Oscillator oscillates at 220 kHz and this signal was modulated by the input AC signal. The AC signal was fed into the reactance modulator circuit through a transformer, which has primary winding with an inductance of 10.65 mH and secondary winding with an inductance of 258.9 mH. The reactance of the primary winding for 10 kHz was 669.6Ω, while the same for

the secondary was 488.01 kΩ. Thus 10 kHz AC signal can easily be passed through the primary winding, but the 300 kHz (LCR meter measurement frequency was 300 kHz) signal was blocked by the secondary winding. The coupling capacitor at point A (Figure 15) was used at 1μF because, at 300kHz, the reactance of the coupling capacitor is 0.53Ω, which is quite low. The output of the FM modulation is shown in Figure 17. The output of the spectrum analyzer (Agilent n9320b) of the FM signal modulated by a 10 kHz input signal in the frequency domain is shown in Figure 17(a), while in Figure 17(b), the FM signal is in the time domain (From Digital Storage Oscilloscope KEYSIGHT DSOX1204G)

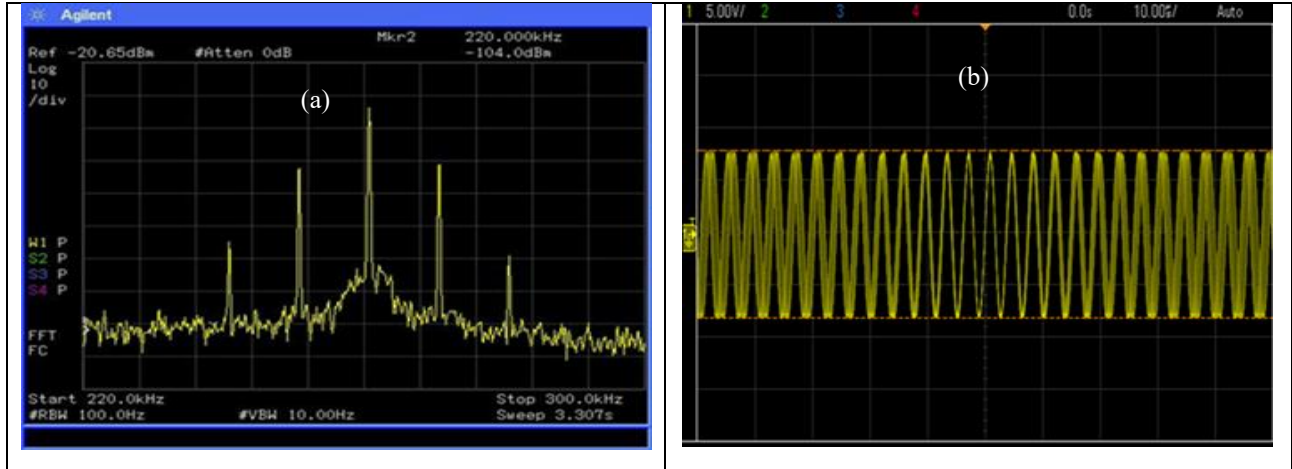


Fig. 17 Output diagram of frequency modulated signal in frequency domain (a) In frequency domain, (b) In time domain.

#### 4. Conclusion

The experimental investigation into the performance of a BJT as a reactance modulator has yielded promising results. It was observed that the BJT could be effectively utilized as a square-law device within the base-emitter voltage range of 0.5 V to 0.75 V. Within this range, the equivalent capacitance of the reactance modulator was linear with the input voltage, which is crucial for achieving optimal performance in frequency modulation applications. Moreover, this range allows the reactance modulator's output to be fed into a Hartley oscillator, facilitating efficient frequency modulation. Experimental observations of frequency modulation in both the time and frequency domains further confirm the viability of using BJTs as reactance modulators. The observed range of

capacitance variation with input voltage for different feedback capacitors reveals its potential for effectively tuning the modulation index in FM modulation applications. These findings enhance our understanding of modulation techniques and pave the way for improved design and implementation of advanced communication systems.

#### Acknowledgments

We would like to acknowledge Satyendra Nath Bose National Centre for basic sciences, Kolkata, West Bengal, India (SNB/NPEP/22-23/279) for supporting financially to carry out the research.

#### References

- [1] Liwei Huang, Yulin Chen, and Hui Huang, "Research of Digital Communication System," *IEEE Conference on Telecommunications, Optics and Computer Science*, Shenyang, China, pp. 257-260, 2020. [[Cross Ref](#)] [[Google Scholar](#)] [[Publisher Link](#)]
- [2] P.M. Grant, and R.S. Withers, "Recent Advances in Analog Signal Processing," *IEEE Transactions on Aerospace and Electronic Systems*, vol. 26, no. 5, pp. 818-849, 1990. [[Cross Ref](#)] [[Google Scholar](#)] [[Publisher Link](#)]
- [3] Alan E. Willner et al., "All-Optical Signal Processing," *Journal of Lightwave Technology*, vol. 32, no. 4, pp. 660-680, 2014. [[Cross Ref](#)] [[Google Scholar](#)] [[Publisher Link](#)]
- [4] George Kennedy, Bernard Davis, and S.R.M. Prasanna, *Electronics Communication Systems*, Tata McGraw-Hill Publishing Co. Ltd., New Delhi, 1985. [[Google Scholar](#)]
- [5] John Douglas Ryder, *Electronic Fundamentals and Applications*, Prentice Hall India Learning Private Limited, 2012. [[Google Scholar](#)]
- [6] Dennis Roddy, and John Coolen, *Electronic Communication*, 4<sup>th</sup> edition, Pearson India, 2008. [[Google Scholar](#)] [[Publisher Link](#)]
- [7] Kosala Herath et al., "A Dual-Signalling Architecture for Enhancing Noise Resilience in Floquet Engineering-Based Chip-Scale Wireless Communication," *IEEE Journal of Selected Areas in Communications*, vol. 42, no. 8, pp. 2039-2053, 2024. [[CrossRef](#)] [[Google Scholar](#)] [[Publisher Link](#)]
- [8] E.H. Armstrong, "A Method of Reducing Disturbances in Radio Signaling by a System of Frequency Modulation," *Proceedings of the Institute of Radio Engineers*, vol. 24, no. 5, pp. 689-740. 1936. [[CrossRef](#)] [[Google Scholar](#)] [[Publisher Link](#)]
- [9] L.J. Giacoletto, "Junction Capacitance and Related Characteristics Using Graded Impurity Semiconductors," *IRE Transaction on Electron Devices*, vol. 4, no. 3, pp. 207-215, 1957. [[CrossRef](#)] [[Google Scholar](#)] [[Publisher Link](#)]
- [10] M.H. Norwood, and E. Shatz, "Voltage Variable Capacitor Tuning: A Review," *Proceedings of IEEE*, vol. 56, no. 5, pp. 788-798. 1968. [[CrossRef](#)] [[Google Scholar](#)] [[Publisher Link](#)]
- [11] H. Funato, A. Kawamura, and K. Kamiyama, "Realization of Negative Inductance Using Variable Active-Passive Reactance (Vapar)," *IEEE Transaction of Power Electronics*, vol. 12, no. 4, pp. 589-596, 1997. [[CrossRef](#)] [[Google Scholar](#)] [[Publisher Link](#)]

- [12] G. Franklin Montgomery, "The Diode Reactance Modulator," *Transactions of the American Institute of Electrical Engineers, Part I: Communication and Electronics*, vol. 77, no. 6, pp. 980-983, 1959. [[CrossRef](#)] [[Google Scholar](#)] [[Publisher Link](#)]
- [13] B.E. Montgomery, "An Inductively Coupled Frequency Modulator," *Proceedings of IRE*, vol. 29, no. 10, pp. 559-563, 1941. [[CrossRef](#)] [[Google Scholar](#)] [[Publisher Link](#)]
- [14] Alexander S. Jurkov, Aaron Radomski, and David J. Perreault, "Tunable Matching Networks Based on Phase-Switched Impedance Modulation," *IEEE Transactions on Power Electronics*, vol. 35, no. 10, pp. 10150-10167, 2020. [[CrossRef](#)] [[Google Scholar](#)] [[Publisher Link](#)]
- [15] Hossein Mashad Nemati et al., "Design of Varactor-Based Tunable Matching Networks for Dynamic Load Modulation of High-Power Amplifiers," *IEEE Transactions of Microwave Theory and Techniques*, vol. 57, no. 5, pp. 1110-1118, 2009. [[CrossRef](#)] [[Google Scholar](#)] [[Publisher Link](#)]
- [16] Transistor Reactance Modulator, DAEnotes, [Online]. Available: <https://www.daenotes.com/electronics/communication-system/transistor-reactance-modulator#:~:text=Reactance%20modulation%20is%20a%20technique,reactance%20of%20a%20specific%20component>
- [17] Mojisola R. Usikalu et al., "Construction of a Mobile Frequency Modulation Transmitter," *4<sup>th</sup> International Conference on Science and Sustainable Development IOP Conference Series: Earth and Environmental Science*, vol. 655, no. 1, 2021. [[CrossRef](#)] [[Google Scholar](#)] [[Publisher Link](#)]
- [18] Yongseok Lim et al., "An Adaptive Impedance-Matching Network Based on a Novel Capacitor Matrix for Wireless Power Transfer," *IEEE Transactions on Power Electronics*, vol. 29, no. 8, pp. 4403-4413, 2014. [[Cross Ref](#)] [[Google Scholar](#)] [[Publisher Link](#)]
- [19] César Sánchez-Pérez et al., "Design and Applications of A 300- 800 Mhz Tunable Matching Network" *IEEE Journal on Emerging and Selected Topics in Circuits and Systems*, vol. 3, no. 4, pp. 531-540, 2013. [[Cross Ref](#)] [[Google Scholar](#)] [[Publisher Link](#)]
- [20] M.B. Chowdary, K. Raj Nutan Satya Sai, and Balajee Maram, "FM transmission Using Single Bipolar Junction Transistor," *Journal of Advancement in Engineering and Technology*, Vol. 7, no. 1, pp. 1-2, 2018. [[Cross Ref](#)] [[Publisher Link](#)]
- [21] Mehdi Azadmehr, Igor Paprotny, and Luca Marchetti, "100 Years of Colpitts Oscillators: Ontology Review of Common Oscillator Circuit Topologies," *IEEE Circuits and Systems Magazine*, vol. 20, no. 4, pp. 8-27, 2020. [[Cross Ref](#)] [[Google Scholar](#)] [[Publisher Link](#)]
- [22] Fan He et al., "Discussion on the General Oscillation Startup Condition and the Barkhausen Criterion," *Analog Integrated Circuits and Signal Processing*, vol. 59, pp. 215-221, 2009. [[Cross Ref](#)] [[Google Scholar](#)] [[Publisher Link](#)]
- [23] Wen-Mei Jiang et al., "New Method of Solving the Oscillation Criterion for Hartley Oscillator," *Iranian Journal of Science and Technology, Transaction of Electrical Engineering*, vol. 45, pp. 1117-1125, 2021. [[Cross Ref](#)][[Google Scholar](#)][[Publisher Link](#)]
- [24] F.B. Llewellyn, "Constant Frequency Oscillators," *Proceedings of the Institute of Radio Engineers*, vol. 19, no. 12, pp. 2061-2094, 1931. [[CrossRef](#)] [[Google Scholar](#)] [[Publisher Link](#)]
- [25] F. A. Record, and J. L. Stiles, "An Analytical Demonstration of Hartley Oscillator Action," *Proceedings of the IRE*, vol. 31, no. 6, pp. 281-287, 1943. [[CrossRef](#)] [[Google Scholar](#)] [[Publisher Link](#)]
- [26] Zhaoyang Zhao et al., "An Overview of Condition Monitoring Techniques for Capacitors in DC-LINK Applications," *IEEE Transactions on Power Electronics*, vol. 36, no. 4, pp. 3692-3716, 2021. [[Cross Ref](#)] [[Google Scholar](#)] [[Publisher Link](#)]